J. Phys. B: At. Mol. Opt. Phys. **32** (1999) 277–286. Printed in the UK PII: S0953-4075(99)93248-0

Ionization cross sections of C_{60} by fast electron impact

A Itoh†, H Tsuchida‡, K Miyabe, T Majima and N Imanishi
Department of Nuclear Engineering, Kyoto University, Kyoto 606-8501, Japan

Received 14 April 1998, in final form 3 November 1998

Abstract. By means of a time-of-flight technique, we have measured cross sections for production of C_{60}^{1-3+} and $C_{58,56}^{2+}$ ions from a gas-phase C_{60} target bombarded by 0.4–5.0 keV electrons. The results were in fairly good agreement with other data at overlapping energies below 1 keV. Semiclassical calculations of the single-ionization cross sections were also performed up to 10 keV using the Deutsch–Märk formula proposed for the C_{60} molecule. A fairly good agreement between the experimental and theoretical cross sections was obtained both in magnitude and in energy dependence. It was found that the double and triple ionization cross sections both decrease monotonically and exhibit no hump structure, indicating that the inner-shell ionization does not play an important role in electron-impact multiple ionization of C_{60}.

1. Introduction

Since the pioneering work of O'Brien *et al* on laser-induced fragmentation of carbon-cluster ions [1], an increasing number of investigations have been performed on the fragmentation and ionization processes of C_{60} molecules by means of a variety of experimental techniques [2–28]. As one of the distinctive properties of C_{60} in comparison with other polyatomic molecules, one should point out the outstandingly high stability of C_{60}^{q+} ions against Coulomb explosion. For instance, Scheier and Märk [8] found multiply charged ions up to $q = 7$ using a Nier-type electron-impact ion source, and Jin *et al* [24] observed ions with a further higher charge state of $q = 9$ in collisions between highly charged slow ions and C_{60}. The latter authors reported that lifetimes are longer than 20 μs for ions with $q < 8$. The multiple ionization and/or multifragmentation of C_{60} can now be commonly observed in heavy ion impact experiments [23–28]. The mass distribution of positively charged ions produced in these collisions exhibits, in general, a bimodal pattern consisting of multiply ionized large-mass ions C_{60-2m}^{q+} ($m = 0, 1, 2, \ldots$) and small fragment ions C_n^+ ($n = 1, 2, 3, \ldots$) caused by multifragmentation. The mechanism leading to such a distribution pattern has, however, not been understood very precisely. This is mainly due to the fact that several different inelastic processes take place between the incident ions and C_{60}; multiple ionization, electron capture/loss, collective excitation, inner-shell ionization followed by Auger relaxation, direct knock-out of constituent atoms and so forth. Consequently, the phenomena get complicated particularly in energetic collisions due to a mixture of these inelastic collisions, and detailed studies on each of these processes have not yet been performed completely.

In contrast, the situation may be essentially simplified when electrons are used as the impact particles. In fact, a number of experimental studies have been performed using electron beams

† E-mail address: itoh@nucleng.kyoto-u.ac.jp
‡ Present address: Department of Physics, Nara Women's University, 630-8506, Japan.

0953-4075/99/020277+10$19.50

in order to determine the fundamental physical quantities of C_{60} such as electron-energy-loss function, ionization potentials or appearance energies of various fragment ions [10–15]. On the other hand, absolute cross sections for ionization of C_{60} have scarcely been reported to date. Baba *et al* [15] measured single-ionization cross sections at an impact energy 38 eV using a Knudsen cell mass spectrometric technique. Vostrikov *et al* [16] measured total single-ionization cross sections from threshold to 70 eV with no mass selection. The comprehensive set of data in a wide range of the impact energy was reported only by a research group led by Märk [17, 18]. They used a two-sector-field mass spectrometer for mass/charge analysis and obtained cross sections for the production of various parent and daughter ions in the impact energy range from threshold to 1 keV.

In the present work the ionization cross sections were measured by means of the time-of-flight (TOF) technique with flight times shorter than about 18 μs for the slowest ions C_{60}^+. The incident electron energy was extended up to 5 keV in order to obtain information about the inner-shell ionization effect in multiple-ionization processes. Calculations of the single-ionization cross sections have also been carried out in the impact energy range from threshold to 10 keV by using the semiclassical formula for the C_{60} molecule proposed by Deutsch *et al* [29].

2. Experimental method

The experimental method and apparatus are similar to those used in our previous work [28] on ion-impact fragmentation of C_{60}. An electron beam from a unipotential-field-type electron gun was collimated to about 1 mm in diameter by an electrostatic einzel lens before entering a crossed-beam collision chamber. The incident energy of the electron beam was varied between 400 eV and 5.0 keV. A C_{60} vapour target was produced by heating a C_{60} powder of 99.98% purity at 450 °C in a temperature-controlled quartz crucible located at the base of the chamber. The effusive C_{60} beam was introduced upward into the electron beam path region through a hole (2 mm in diameter) opened at the top of the crucible. The incident electron beam axis was 35 mm high from the hole. Under this geometrical condition the effusive target beam was not collimated but was considered to distribute rather uniformly in the collision region. The mass-to-charge distribution of fragment ions produced in collisions between incident electrons and C_{60} was measured with a TOF spectrometer located perpendicular both to the electron beam and target effusive directions. As described in [28], the TOF spectrometer consists of an extraction region, an acceleration region and a drift region in conjunction with a two-stage multichannel plate (MCP) detector (40 mm in diameter). The spectrometer was operated under a Wiley–McLaren spatial-focusing condition [30]. Secondary electrons produced simultaneously in the same collisions were used as start trigger pulses for TOF measurements. Extraction of ions and electrons was made by applying $\pm$250 V to two Mo-mesh grids separated by 40 mm so as to keep the electron beam axis at the earth potential. The size of these grids was 60 and 50 mm in the horizontal (beam axis) and vertical directions, respectively. Extracted electrons were then further accelerated by another Mo-mesh grid set to 1 kV and finally detected by a two-stage MCP detector (20 mm in diameter). To avoid detection of unnecessary multiply scattered electrons, the electron flight part was shielded by a cylindrical stainless-steel tube. The TOF spectra of fragment ions were obtained by a fast-multichannel scaler (FMCS, LN-6500, Labo) with the highest time resolution of 1 ns enabling us to detect multiple ions produced in a single collision. In the present experiment the FMCS was operated with a time resolution of 8 ns/channel in 4096 total channels. The flight time of the slowest C_{60}^+ ions was about 18 μs.

Production cross sections σ of a fragment ion are related to its peak intensity Y in a form $Y = \sigma I_0 N L G T F O f$, where I_0 is the incident beam flux, N the target density, L the effective

target length, G the total transmission of grids (0.55), T the collection efficiency of the TOF spectrometer, F the relative detection efficiency of the MCP, O the MCP open area ratio (0.57) and f the total detection efficiency for the start electrons. In the present work the incident electron beam current was too weak to be measured correctly, so that the ionization cross sections of C_{60} were determined indirectly. Namely, a small quantity of N_2 gas was introduced through a gas-leak valve into the collision chamber uniformly as a reference target gas during C_{60} evaporation. The introduced N_2 gas pressure P_N was about 2.0×10^{-6} torr measured by a calibrated B-A gauge mounted near the collision region. Peak intensities were measured for nitrogen ions of N_2^+, N^+ and N^{2+} originating from ionization and dissociation of N_2 molecules. The total sum Y_N of these intensities multiplied by their charges correspond to total ionization cross sections σ_N of N_2, for which experimental data are available in the literature [31, 32]. With this normalization method all the commonly appearing quantities as well as I_0, G and O are cancelled out as will be described below, and the cross sections may be obtained by

$$\sigma \simeq \sigma_N \frac{Y P_N F_N}{Y_N P_C F}$$

where P_C is the pressure of C_{60} and F_N is the detection efficiency for nitrogen ions.

The collection efficiency T representing an ion-arrival efficiency at the MCP front plate depends on initial kinetic energies and emission angles of the ions. Using a peak profile analysis described in [28] initial kinetic energies of $C_{60}^{(1-3)+}$ and nitrogen ions were deduced from the spectrum observed (see figure 1). The results were substantially small, of order below 0.1 eV. As discussed in [28] nearly 100% of such low-energy ions can, independently of their emission angles, be extracted parallel with the TOF axis by the extraction field of 125 V cm^{-1} used here. Consequently, we can put $T \simeq 1$ for both C_{60}^{q+} and nitrogen ions. The observation length seen by the MCP for these low-energy ions is about the same as the MCP detection size (40 mm).

Similarly, the detection efficiency f for start electrons depends on grid transmission (0.67 in total), MCP open area ratio (0.57) and on initial electron energy which was unknown in this experiment. Bolorizadeh and Rudd [33] measured the energy distribution of secondary electrons down to 2 eV for collisions between 50 eV–2 keV electrons and H_2O molecules. One can see in their paper that the energy distribution is dominated by low-energy electrons of a few eV and agrees quite well with theoretical predictions indicating a peak maximum at 0 eV. Thus, it may be plausible to assume a similar distribution peaking at about 0 eV for both molecules of C_{60} and N_2. With this assumption the total efficiency f is regarded to be the same for both molecules. It might, however, be possible that the distribution may be slightly different for both cases. In order to estimate an uncertainty the collection efficiency T for the electron extraction part was calculated for several electron energies using a similar ray-tracing simulation to [28]. For simplicity the calculations were made along a 20 mm long beam axis, the size of the MCP detection diameter. The T values obtained were unity, 0.85 and 0.77 for electron energies of 0, 2 and 5 eV, respectively. Hence the uncertainty arising from f is estimated to be 10–20%. As for the observation length of the MCP, it is not simply determined because it depends on the electron energy. For instance, 17% of such electrons are expected to reach the detector that were emitted 4 mm outside the detection window with an energy of 2 eV. However, it should be emphasized that the majority of these slow electrons detected by the MCP are the electrons emitted within the MCP detection window. Thus, we adopted 20 mm as the observation length of the present experiment.

The target density of C_{60} was calculated from vapour pressure data reported by Abrefah *et al* [34], taking account of the present experimental geometry. Since the C_{60} beam was obtained from a single tiny hole in the crucible, the diffusion of C_{60} molecules into the collision region can be considered to follow Knudsen's cosine law distribution. Calculations showed

a rather flat pressure distribution along the electron beam axis. For instance, the pressure difference was estimated to be only 11% within the observation length of 20 mm. Thus, the effective target length L for C_{60} and N_2 is expected to be the same to within an error of 11%. The averaged target pressure P_C was 3.2×10^{-7} torr with a vapour pressure of 1.3×10^{-4} torr inside the crucible at a temperature of 450 °C [34].

The detection efficiency F of the MCP for various fragment ions was obtained by our different experiment using heavy ion impacts, for which a detailed description will be given in our forthcoming paper. Briefly, the intensity variation of fragment ions was measured as a function of impinging energy (2–20 keV) on the MCP front plate by changing the voltage to the front plate, and a smooth fitting curve connecting a set of data was determined. An expression for F obtained for C_{60}^{q+} ions with impinging energy E (keV) was $-100\ln(1-F) = 1.48E + 2.18E^2$. Here, a plateau observed at the higher energy side was taken to be unity. In the present experiment the front voltage was -4 kV, giving rise to impinging energies of $4q$ keV for ions with charge q. The relative detection efficiencies F were, therefore, 0.34, 0.78 and 0.96 for C_{60}^{+}, C_{60}^{2+} and C_{60}^{3+} ions, respectively. As for the light fragment ions such as C^+ and C_2^+ moving much faster than any C_{60}^{q+} ions, the intensity change was not observed within statistical errors, indicating $F \simeq 1$. This was also the case for the nitrogen ions; $F_N \simeq 1$. Note that the present F values given by the above formula are very close to those reported in [23].

The cross sections σ_N obtained by the condenser method are reported by Rapp and Englander-Golden [31] for impact energies 16 eV–1 keV and by Schram *et al* [32] for 100 eV–20 keV. The experimental accuracy of these cross sections is a few per cent. The latter cross sections are, however, systematically smaller than the former ones in the overlapping region, so that above 1 keV we used the latter data normalized at 1 keV by multiplying by 1.18. The σ_N used in the present work are listed in table 1.

Among all the uncertainties involved in the quantities described above, the largest systematic error comes from the P_C value determined with the vapour pressure data which have a substantial scatter in the literature [34–36]; e.g. 8.6×10^{-5} [35], 3.1×10^{-4} [36] and 1.7×10^{-4} torr [36] at 450 °C. Therefore, the systematic error of the present cross sections is assumed to be a factor of more than two, while an overall experimental error arising from other quantities was about 20%.

Table 1. Cross sections (in units of 10^{-16} cm^2) for the production of C_{60}^{+}, C_{60}^{2+}, C_{60}^{3+} and C_{58}^{2+} ions by electron impact. σ_N represents total ionization cross sections of N_2 gas [31, 32] used in the present normalization method. Experimental errors of the present data are about 20%, while the total systematic uncertainty is assumed to be a factor of two (see text).

Electron energy (keV)	C_{60}^{+}	C_{60}^{2+}	C_{60}^{3+}	C_{58}^{2+}	σ_N
0.4	20.5	4.14	0.624	0.500	1.66
0.5	19.4	3.42	0.506	0.358	1.45
0.6	17.7	3.06	0.362	0.230	1.29
0.8	15.6	2.42	0.261	0.165	1.06
1.0	14.6	1.93	0.208	0.134	0.923
2.0	8.29	0.932	0.100	0.0347	0.542
3.0	7.08	0.579	0.0513	0.0170	0.387
4.0	5.13	0.371	0.0365	0.0125	0.309
5.0	3.73	0.331	0.0307	0.0113	0.259

3. Results and discussion

Figure 1 shows an example of TOF spectra of a mass/charge distribution obtained at 500 eV electron impact. Observed in the spectrum are singly through triply ionized parent ions C_{60}^{1-3+} and some fragment daughter ions arising through loss of even-numbered carbon atoms. Due to somewhat poor signal count statistics, more than fourfold ionized species could not be detected clearly in the present work. In the low-mass region where small carbon fragment ions are expected, a 'continuous' broad structure of background type is observed. At the present stage, however, we cannot make clear its origin—whether the structure is a result of superposition of real carbon fragment ions or not. Apart from this continuous part, the spectrum is dominated by sharp lines originating from the additionally introduced N_2 gas and impurity gases. It should be pointed out that the intensities of N^+ and N^{2+} ions formed by dissociative ionization were found to be smaller than several per cent of the N_2^+ ions, implying that in the present energy range the dominant part of the total ionization cross section (σ_N) is the N_2^+ production cross section.

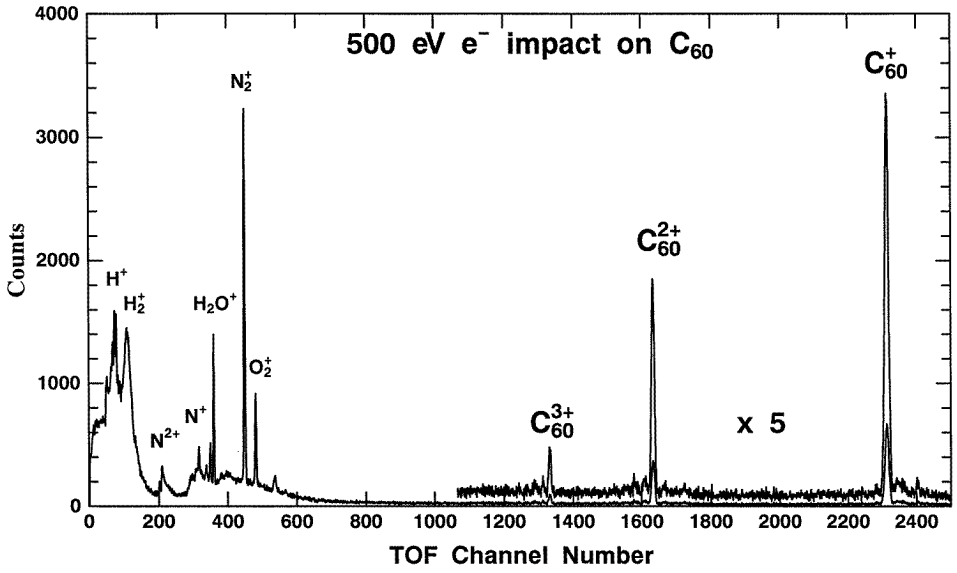

Figure 1. Time-of-flight spectrum of positively charged ions produced in collisions of 500 eV electrons with a C_{60} vapour target.

One can see that C_{60}^{q+} ions as well as N_2^+ ions exhibit fairly narrow and symmetric peak profiles, implying small initial kinetic energies as described in the previous section. The symmetric shape of parent ions C_{60}^{q+} indicates that delayed fragmentation processes such as $C_{60}^{q+} \rightarrow C_{58}^{q+} + C_2$ are negligible within the time scale (a few microseconds) of this experiment. This is because, if such delayed processes occur during flight before entering the field-free region, the profile should appear to be asymmetrical with tailing in faster TOF side. Indeed, such delayed processes are expected to become more significant in long time scale experiments as shown by Foltin *et al* [9]. Therefore, peak intensities measured for the parent ions can be regarded as correctly reflecting the original intensities within our experimental errors. This fact also implies that a contribution from delayed processes of parent ions is of little importance to the formation of daughter ions.

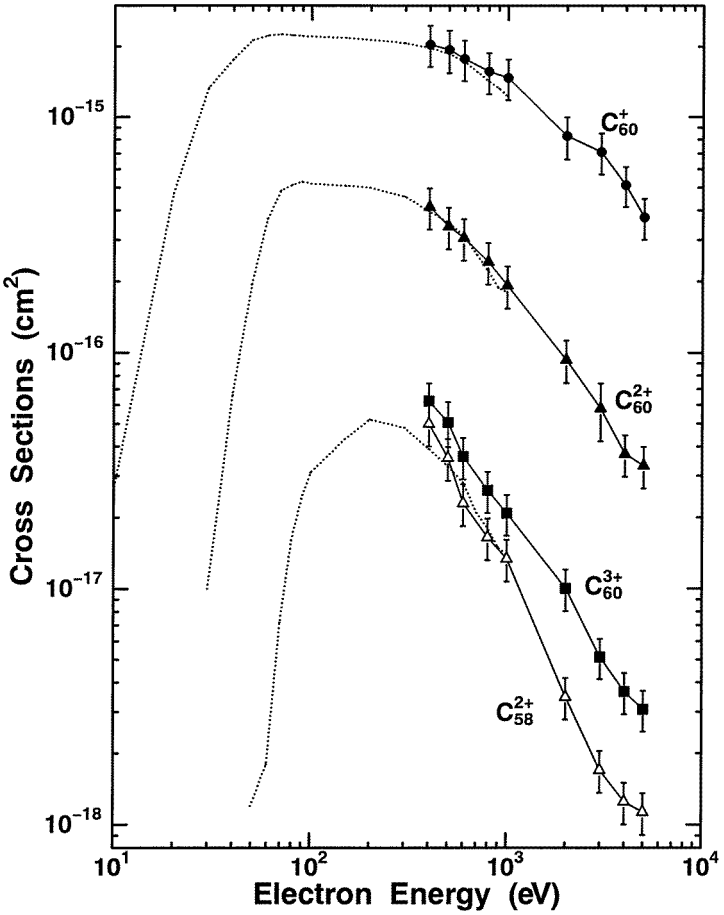

Figure 2. Experimental cross sections for the production of $C_{60}^{1,2,3+}$ and C_{58}^{2+} ions. The dotted curves are taken from [17, 18]. The experimental errors of the present values are mainly due to counting statistics.

The production cross sections σ_q for C_{60}^{q+} ($q = 1$–3) ions are listed in table 1 and plotted in figure 2. As for the daughter ions we could obtain the cross sections only for C_{58}^{2+} and C_{56}^{2+} ions due to poor counting statistics. Since the cross sections for these two daughter ions were found to be nearly equal within the experimental errors, only the data for C_{58}^{2+} are presented in table 1 and figure 1. The double- and triple-ionization cross sections $\sigma_{2,3}$ are smaller than the single-ionization cross sections σ_1 by roughly one and two orders of magnitude, respectively, when compared at 5 keV. The cross sections for daughter ions C_{58}^{2+} are comparable in magnitude with those for C_{60}^{3+} at low impact energies and decrease more steeply with increasing impact energy, indicating that the excess excitation leading to C_{2m} emission becomes less important at higher impact energies. Qualitatively, the relationship of the magnitude between the present cross sections coincides fairly well with that of the appearance energies of these ions [14], which are 7.6, 19, 35.6, 54 and 59.8 eV for C_{60}^+, C_{60}^{2+}, C_{60}^{3+}, C_{58}^{2+} and C_{56}^{2+}, respectively.

Experimental data below 1 keV measured by Märk's group [17, 18] are also shown in figure 2, where the cross sections $\sigma_{1,2,3}$ are compared. Note that our relative cross sections can be discussed within an error of 20%, although the absolute values have a large systematic

uncertainty of a factor of more than two. One can see that the present results are in fairly good agreement with their data in the overlapping energy range 0.4–1.0 keV, while our σ_3's are slightly larger by about 30%. This discrepancy may be attributed to different time scales of the flight times used in the two experiments. In their experiments a two-sector-field mass spectrometer was used, and as mentioned in their papers the detection of ions suffered from counting loss due to metastable dissociation decay during flight from the ion source region to the detector. Such an effect would become more significant with increasing degree of ionization q [9]. On the stability of multiply charged C_{60}^{q+} ions Jin *et al* [24] reported that lifetimes are longer than 20 μs for $q < 8$. In our TOF experiments the flight times of these ions ranges from about 10 μs for C_{60}^{3+} to 18 μs for C_{60}^{+} ions. Therefore, the delayed fragmentation may occur predominantly in the field-free drift region of our TOF spectrometer, which however does not affect the signal counting as well as the peak profile. It should be noted that their revised σ_3 cross sections [37] are in fairly good agreement with the present values.

Although a full quantum mechanical formalism is not available for polyatomic molecules such as C_{60}, Deutsch *et al* [29] have recently proposed an easy-to-apply semiclassical formula to calculate single-ionization cross sections of C_{60} by extending their DM formalism originally applied for atoms, molecules and clusters [38–40]. In this DM formalism, the outermost 120 molecular orbitals of C_{60} are represented as a linear combination of atomic C(2s) and C(2p) orbitals. The single-ionization cross section σ_{DM} is given by

$$\sigma_{\mathrm{DM}} = \sum_{nl} g_{nl}\pi r_{nl}^2 \xi_{nl} f(u)$$

$$f(u) = \frac{1}{u}\left(\frac{u-1}{u+1}\right)^a \left(1 + \left(1 - \frac{1}{2u}\right)\ln\left(2.7 + \sqrt{u-1}\right)\right)$$

where r_{nl}^2 is the mean square radius of the nl-shell, ξ_{nl} is the number of electrons in the nl-shell, g_{nl} is the weighting factor and $u = E/E_{nl}$ is the ratio between the incident electron energy and the binding energy of the nl-shell. The power a is $\frac{7}{4}$ and 2 for the s- and p-shell, respectively, and the weighting factor g_{nl} is obtained by $g_{nl}E_{nl} = 20$ and 30 eV for 2s and 2p electrons, respectively [41]. The calculated results are shown in figure 3, where the total sum (denoted by DM) of individual cross sections for the nl-shells and two examples of the nl cross sections ($6h_u$ and $2a_g$) are depicted.

The state $6h_u$ represents the highest occupied molecular orbital ($E_{nl} = 8.14$ eV) with fivefold (ten electrons) degeneracy and is essentially the pure atomic 2p orbital, and the state $2a_g$ ($E_{nl} = 35.70$ eV) with one degeneracy is the lowest state of the outer 120 orbitals. The cross sections for other orbitals lie between the two curves. The total DM cross sections deviate largely from our experimental values (σ_1) throughout the impact energy range. As pointed out in [29], however, half the calculated values should be compared with the experimental values because of an argument that for the incident electron only about half of the 60 C atoms contribute to the cross sectional area 'seen' by the projectile. The cross sections denoted by DM/2 in figure 3 are half the original values. Obviously these theoretical values are in much better agreement with the experimental data.

Concerning the production mechanism of multiply charged ions, it can in general be stated that these ions are formed predominantly through simultaneous or successive ionization of multiple electrons from the outer shells containing 240 electrons. This is readily understandable because the appearance energies [14] for C_{60}^{q+} ions are much smaller than the 1s binding energy. It is, however, interesting to investigate a contribution from ionization of 120 1s electrons, since the 1s ionization is expected to take place preferentially in the present impact energy range. In addition, if inner-shell ionization occurs, then it may cause to some extent an increase in the production of multiply charged ions due to the Auger effect. For this purpose we plotted

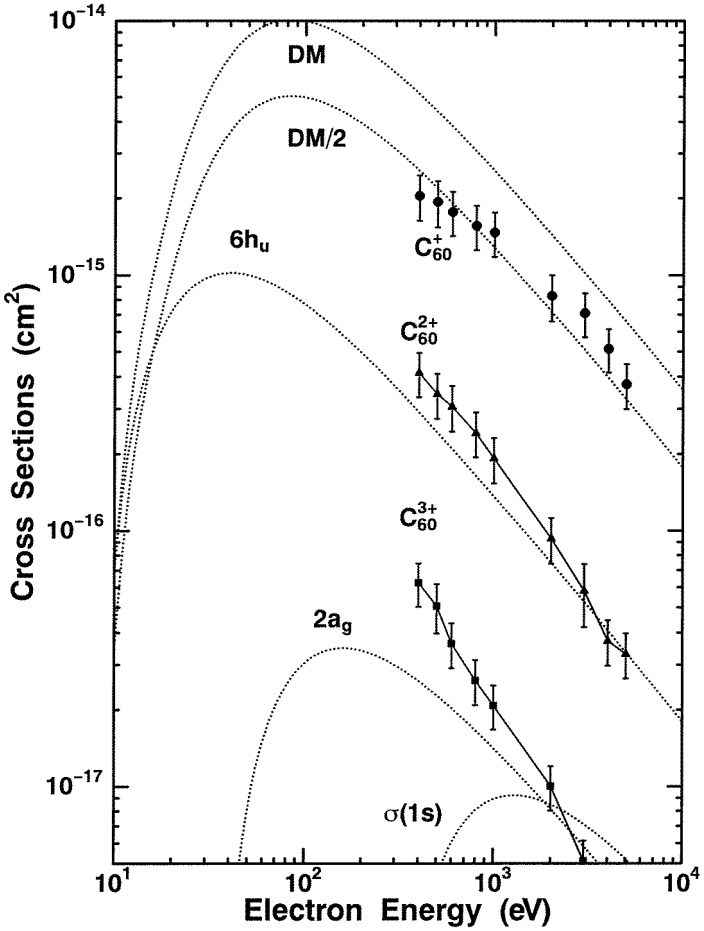

Figure 3. Comparison of the present single-ionization cross sections with semiclassical calculations from the DM formula [29, 42]. The curve DM is the original cross sections, the curve DM/2 represents half the original values, and the curves $6h_u$ and $2a_g$ correspond to outermost and innermost molecular orbitals out of the 120 outer shells of C_{60}. The curve $\sigma(1s)$ represents the 1s ionization cross sections taken from [42] (see text).

in figure 3 the ionization cross sections of carbon 1s electrons calculated by Deutsch *et al* [42] using the above DM formula with $g_{1s}E_{1s} = 70$ eV and $E_{1s} = 288$ eV. Note that the plotted cross sections $\sigma(1s)$ are 30 times the original atomic cross sections for the reason described above. The cross sections have a peak maximum around 1.3 keV, which is as expected considerably higher than those of other orbitals. On the other hand, the magnitude is smaller than 1% of $\sigma_{DM}/2$, and about 6% of the experimental values σ_2 at the peak energy. Moreover, the energy dependence of $\sigma(1s)$ is significantly different from the experimental data. By assuming the cross sections to have a form $\sigma \sim E^{-p}$ above the corresponding peak energies, the slopes p were obtained as 0.87 (σ_1), 1.1 (σ_2), 1.2 (σ_3), 0.84 (σ_{DM}) and only 0.60 for $\sigma(1s)$. Note an equivalent p value for σ_1 and σ_{DM}. It should be emphasized that the experimental cross sections $\sigma_{2,3}$ do not exhibit any hump structure around the $\sigma(1s)$ peak area. Thus, we conclude that the inner-shell ionization does not play an important role in multiple ionization of C_{60}.

4. Conclusions

The time-of-flight mass/charge distributions of positively charged ions have been measured for the C_{60} vapour target bombarded by fast electrons with energies of 0.4–5 keV. Absolute cross sections for the production of parent and daughter ions were obtained by the normalization method using ionization cross sections of N_2 gas available in the literature [31, 32]. The present cross sections were in fairly good agreement with other experimental data [17, 18, 37] and also with the semiclassical calculations [29]. It was found that the magnitudes of the cross sections varied similarly to those of the appearance energies [14] of the corresponding ions. For all the cross sections the energy dependence was rather monotonic and did not exhibit any hump structure around the peak area of the 1s ionization cross sections [42]. Thus, the contribution from the inner-shell ionization is negligibly small in the electron-impact ionization of C_{60}.

Acknowledgments

The authors would like to acknowledge stimulating discussions with Professor T D Märk, and thank M Imai, K Yoshida, K Norizawa and students of our group for their help during the experiment.

References

[1] O'Brien S C, Heath J R, Curi R F and Smalley R E 1988 *J. Chem. Phys.* **88** 220–30
[2] Radi P P, Bunn T L, Kemper P R, Moichan M E and Bowers M T 1987 *J. Chem. Phys.* **88** 2809–14
[3] Hertel I V, Steger H, de Vries J, Weisser B, Menzel C, Kamke B and Kamke W 1992 *Phys. Rev. Lett.* **68** 784–7
[4] Aksela S, Nõmmiste E, Jauhiainen J, Kukk E, Karvonen J, Berry H G, Sorensen L L and Aksela H 1995 *Phys. Rev. Lett.* **75** 2112–5
[5] Lykke K R 1995 *Phys. Rev.* A **52** 1354–7
[6] Hohmann H, Ehich R, Furrer S, Kittelmann O, Ringling J and Campbell E E B 1995 *Z. Phys.* D **33** 143–51
[7] Hunsche S, Starczewski T, L'Huillier A, Persson A, Wahlström C-G, van Linden van den Heuvell B and Svanberg S 1996 *Phys. Rev. Lett.* **77** 1966–9
[8] Scheier P and Märk T D 1994 *Phys. Rev. Lett.* **73** 54–7
[9] Foltin M, Echt O, Scheier P, Dünser B, Wörgötter R, Muigg D, Matt S and Märk T D 1997 *J. Chem. Phys.* **107** 6246–56
[10] Luffer D R and Schram K H 1990 *Rapid Commun. Mass Spectrom.* **4** 552–6
[11] Srivastava S K, Jong G, Leifer S and Saunders W 1993 *Rapid Commun. Mass Spectrom.* **7** 610–3
[12] Keller J W and Coplan M A 1992 *Chem. Phys. Lett.* **193** 89–96
[13] Foltin M, Lezius M, Scheier P and Märk T D 1993 *J. Chem. Phys.* **98** 9624–34
[14] Wörgötter R, Dünser B, Scheier P and Märk T D 1994 *J. Chem. Phys.* **101** 8674–9
[15] Baba M S, Narasimhan T S L, Balasubramanian R and Mathews C K 1992 *Int. J. Mass Spectrom. Ion Proc.* **114** R1–8
[16] Vostrikov A A, Dubov D Yu and Agarkov A A 1995 *Tech. Phys. Lett.* **21** 715–6
[17] Dünser B, Lezius M, Scheier P, Deutsch H and Märk T D 1995 *Phys. Rev. Lett.* **74** 3364–7
[18] Matt S, Dünser B, Lezius M, Deutsch H, Becker K, Stamatovic A, Scheier P and Märk T D 1996 *J. Chem. Phys.* **105** 1880–96
[19] Hvelplund P, Andersen L H, Haugen H K, Lindhard J, Lorents D C, Malhorta R and Ruoff R 1992 *Phys. Rev. Lett.* **69** 1915–8
[20] Völpel R, Hofmann G, Steidl M, Stenke M, Schlapp M, Trassl R and Salzborn E 1993 *Phys. Rev. Lett.* **71** 3439–41
[21] Shen H, Hvelplund P, Mathur D, Bárány A, Cederquist H, Selberg N and Lorents D C 1995 *Phys. Rev.* A **52** 3847–51
[22] Ehlich R, Westerburg M and Campbell E E B 1996 *J. Chem. Phys.* **104** 1900–11
[23] Walch B, Cocke C L, Voelpel R and Salzborn E 1994 *Phys. Rev. Lett.* **72** 1439–42
[24] Jin J, Khemliche H, Prior H and Xie Z 1996 *Phys. Rev.* A **53** 615–8

[25] Briand J-P, de Billy L, Jin J, Khemliche H, Prior M H, Xie Z, Nectoux M and Schneider D H 1996 *Phys. Rev. Lett.* **53** R2925–8
[26] Cheng S, Berry H G, Dunford R W, Esbensen H, Gemmel D S, Kanter E P and LeBrun T 1996 *Phys. Rev.* A **54** 3182–94
[27] Nakai Y, Itoh A, Kambara T, Bitoh Y and Awaya Y 1997 *J. Phys. B: At. Mol. Opt. Phys.* **30** 3049–58
[28] Itoh A, Tsuchida H, Miyabe K, Imai M and Imanishi N 1997 *Nucl. Instrum. Methods* B **129** 363–8
[29] Deutsch H, Becker L, Pittner J, Bonacic-Koutecky V, Matt S and Märk T D 1996 *J. Phys. B: At. Mol. Opt. Phys.* **29** 5175–81
[30] Wiley W C and McLaren I H 1955 *Rev. Sci. Instrum.* **26** 1150–7
[31] Rapp D and Englander-Golden P 1965 *J. Chem. Phys.* **43** 1464–79
[32] Schram B L, De Heer F J, Van der Wiel M J and Kistemaker J 1995 *Physica* **31** 94–112
Schram B L, Moustafa H R, Schutten J and De Heer F J 1996 *Physica* **32** 734–40
[33] Bolorizadeh M A and Rudd M E 1986 *Phys. Rev.* A **33** 882–7
[34] Abrefah J, Olander D R, Balooch M and Siekhaus W J 1992 *Appl. Phys. Lett.* **60** 1313–4
[35] Mathews C K, Sai Baba M, Lakshmi Narasimhan T S, Balasubramanian R, Sivaraman N, Srinivasan T G and Vasudeva Rao P 1992 *J. Phys. Chem.* **96** 3566–8
[36] Piacente V, Gigli G, Scardala P, Giustini A and Ferro D 1995 *J. Phys. Chem.* **99** 14 052–7
[37] Tarnovsky V, Kurnczi P, Matt S, Märk T D, Deutsch H and Becker K 1998 *J. Phys. B: At. Mol. Opt. Phys.* **31** 3043–8
[38] Deutsch H and Märk T D 1987 *Int. J. Mass Spectrom. Ion Proc.* **79** R1–8
[39] Margreiter D, Deutsch H, Schmidt M and Märk T D 1990 *Int. J. Mass Spectrom. Ion Proc.* **100** 157–76
[40] Deutsch H, Becker K and Märk T D 1995 *Int. J. Mass Spectrom. Ion Proc.* **144** L9–12
[41] Margreiter D, Deutsch H and Märk T D 1994 *Int. J. Mass Spectrom. Ion Proc.* **139** 127–39
[42] Deutsch H, Margreiter D and Märk T D 1994 *Z. Phys.* D **29** 31–7